ROBUST REAL-TIME MR-GEOMETRIC DISTORTION CORRECTION FOR INTERVENTIONAL PROCEDURE ON MOBILE TARGETS

B. Denis de Senneville[1,2]*, M. Ries*[2]*, C.T.W. Moonen*[2]*,*

[1] Institut de Mathématiques de Bordeaux (IMB)
UMR 5251 CNRS/Université Bordeaux 1/INRIA, F-33400 Talence, France
[2] Imaging Division, UMC Utrecht, Utrecht, Netherlands
{b.desenneville,m.ries,c.moonen}@umcutrecht.nl

ABSTRACT

Rapid dynamic MR-imaging can provide both functional and positional informations in real-time, which can be used to retroactively control an interventional procedure. Although rapid echo-planar imaging (EPI) is frequently used in this role, EPI often suffers from geometric distortions. These signal localization errors are caused by spatial magnetic field inhomogeneities induced by magnetic suceptibility variations within the human body and instrumental limitations of the acquisition system. This type of artifact can be addressed by mapping and converting the spatial magnetic field inhomogeneities a priori into a pixel shift and to subsequently correct the EPI-images. Furthermore, for real time guidance of interventions in organs subject to periodical physiological motion, the correction needs to account for time variant changes of the magnetic field during the motion cycle.

The correction described in this paper consists of two steps: A parameterized model of the motion induced magnetic field perturbation is computed in a preparative step; subsequently, during the intervention, this model is used to reconstruct the magnetic field perturbation corresponding to the actual organ position in real-time, which in turns allows computation of distortion corrected MR-images.

***Index Terms*—** Magnetic Resonance Imaging, Real time systems, Motion analysis.

1. INTRODUCTION

In interventional procedures, such as catheter tracking, biopsies or thermal ablations [1], Magnetic Resonance Imaging (MRI) is widely used to provide functional and/or positional informations. The recent developments in rapid MR-sequences, associated with fast data processing strategies, now allow to obtain those informations with both high frame-rates and low image latencies [2]. This facilitates the use of MRI to retroactively control the interventional procedure in real-time [3]. MRI can provide continuous mapping of the target anatomy in the human body as well as the local magnetic field by exploiting the complex nature of the MR-signal: whereas the signal magnitude of gradient recalled sequences [4] provides anatomical information such as the position and the composition of the tissue, the phase φ is directly proportional to the local magnetic field. A variety of MR-sequences are commonly used for rapid MR-imaging and many rely on a gradient recalled echo-planar readout train for the rapid data acquisition [5] [6]. However, echo-planar images are prone to geometric distortions due to the large acquisition bandwidth, which amplifies the effect of static magnetic field inhomogeneities, susceptibility changes, eddy-current effects and gradient non-linearities [7]. These distortions are highly undesirable if the MR-images are used for remoting interventional devices, which requires a precise relation between the target position in the image and its true position in 3D space [8]. Several geometric distortion correction techniques for echo-planar images have been proposed in the past such as [9] [10]. One approach consists of converting the magnetic field map (ΔB_0) into a pixel shift in the phase-encoding direction (Δy) according to the following equation [11] [12]:

$$\Delta y = \frac{\gamma.\Delta B_0}{BW_{pe}} \tag{1}$$

where γ is the gyromagnetic ratio ($\approx$ 42.58 MHz/Tesla) and BW_{pe} the bandwidth per pixel in the phase encode direction. The field map ΔB_0 can be determined by collecting gradient echo images with two different echo time (TE) values (noted TE_1 and TE_2). After calculation of the phase maps from each image (noted φ_{TE_1} and φ_{TE_2}), ΔB_0 can be obtained as follows:

$$\Delta B_0 = k.(\varphi_{TE_2} - \varphi_{TE_1}), \qquad k = \frac{1}{2\pi.\gamma.(TE_2 - TE_1)} \tag{2}$$

This method has recently been extended for the dynamic real-time correction of geometric distortions for either static or mobile organs in [13]: The challenge in this approach is the requirement to dynamically update ΔB_0 in order to compensate for dynamic changes induced by physiological motion or the displacement of interventional devices. This can be achieved by continuously alternating the echo-time of a gradient-recalled echo-planar sequence between the two values TE_1 and TE_2. ΔB_0 at instant n was calculated using a temporal window of 3 dynamics, as follows:

$$\Delta B_0 = k.\left(\varphi_{TE_2}(n) - \frac{\varphi_{TE_1}(n-1) + \varphi_{TE_1}(n+1)}{2}\right) \tag{3}$$

Note the linear interpolation between the phases ($\varphi_{TE_1(n-1)}$ and $\varphi_{TE_1(n+1)}$) of two consecutive images with the same TE. Although this linearly interpolated value introduces a latency of one image in the correction, it also gives a more accurate representation of the pixel shift at instant n. This method can be classified as a "direct" approach since does not require additional acquisitions, and all the acquired images are directly used to correct for geometric distortions on the fly. However, this approach imposes severe restrictions

The author would like to thank the European Research Council (project ERC-2010-AdG-20100317, Sound Pharma) and the Foundation InNaBioSanté (project ULTRAFITT) for funding.

on the imaging protocol since a rapid acquisition sequences is required compared to the observed motion. To address the later, an alternative method is here proposed, which can be classified as an "indirect" approach since it is based the two following steps: First, in a preparative step a magnetic field perturbation model is established, which relates field changes with motion. Subsequently, during the intervention, this model is used in real time to reconstruct the magnetic field perturbation ΔB_0 corresponding to the current organ position. This allows to compute in the final step with Eq. (1) distortion free EPI-images. The method is evaluated in-vivo on a free breathing human volunteer. Intrinsic advantages and drawbacks of "direct" and "indirect" approaches are then compared and discussed.

2. METHOD DESCRIPTION

2.1. Preparative learning step

During the preparative learning step prior to the intervention, dynamic field mapping was performed during the motion cycle of the organ. This was achieved by acquiring continously a rapid gradient-recalled echo-planar images with two alternating echo-times TE_1 and TE_2 over several motion cycles. During the acquisition, the images are split in two image collections of $N = 100$ images for each echo time. For abdominal organs with a typical respiration frequency of 3-5 seconds, the use of imaging frame rates of 10 images per second allows to complete the acquisition of the collection in 20 seconds.

The magnitude images in each collection are subsequently compared to a pre-selected reference image of the target area by selecting the image acquired at the apex of the exhalation phase as the reference image $M^{Ref}_{TE_1}$ and $M^{Ref}_{TE_2}$ for each collection. Subsequently, for both image collections a linear relation between the variation of the phase signal and the target displacement was established similar to the approach proposed by [14]:

1. A training set of N motion vector fields relating the current target position in each image with the reference position $M^{Ref}_{TE_1}$ and $M^{Ref}_{TE_2}$ was obtained for both collections, using an optical-flow based image registration algorithm [15]. The implemented approach was originally proposed by Horn&Schunck [16] for optical image stabilization and computs a displacement field on a pixel-by-pixel basis. A multi-resolution scheme was used [17] in order to optimize the computation time and to stabilize the convergence of the algorithm.

2. Due to the oversampling of the physiological motion-cycle, both sets of motion vector fields are sparse and a reduced parameterized motion flow model D^i, $0 \leq i < K \ll N$ was constructed using Principal Components Analysis. The spatial transformation T_t at instant t between the actual anatomical image (noted $M^t_{TE_j}$, $j = \{1, 2\}$) and the reference could be expressed as a linear combination of the computed basis vector fields B^i as follows:

$$T_t(x, y) = \sum_{i=0}^{K-1} D^i_t B^i(x, y) \tag{4}$$

Whereby the eigenvectors B^i were ordered according to their corresponding eigenvalues. The threshold value for K, which separates eigenvectors representing physiological motion ($i \leq K$) and from eigenvectors coding for noise contribution ($i > K$) was determined using the method proposed in [14]: Since the respiratory and the cardiac activities are periodic, D^i_t ($\forall t$, $0 \leq t < N$) was analyzed in the Fourier domain. Typical periods of the respiratory and cardiac activities are, in the general case, in the range of 0.15-0.3Hz and 0.5-2Hz, respectively. A threshold of 4 Hz was used to separate contributions from physiological motion from noise. The reduced set of parameters D^i_t, which gives a representation of the organ deformation only due to physiological motion, can then be computed by minimizing Eq. (5) using a Marquardt-Levenberg least square solver.

$$LS = \left(M^{ref}_{TE_j} - T_t^{-1}(M^t_{TE_j})\right)^2, j = \{1, 2\} \tag{5}$$

3. The overall phase variation could be approximated by a sum of linear phase changes of each principal motion component on a pixel-by-pixel basis, as shown in Eq. (6). For that purpose, the obtained motion field was used to remap all pixels of the phase images to their reference position. P^i, $0 \leq i < K$, which denotes the parameterized phase model, is computed at the end of the preparative step, using a Singular Value Decomposition (SVD) applied on the overdetermined set of N equations and $K + 1$ unknowns:

$$T^{-1}\left(\varphi_t(x, y)\right) = \sum_{i=0}^{K-1} D^i_t P^i(x, y) + P^K(x, y), 0 \leq t < N, \tag{6}$$

whereby $P^K(x, y)$ represents the static phase offset.

Using $P^i_{TE_1}$ and $P^i_{TE_2}$ ($0 \leq i \leq K$) as the corresponding parameterized phase model for each collection the overall parameterized magnetic field model can be derived as follows:

$$\Delta B^i_0(x, y) = k.\left(P^i_{TE_2}(x, y) - P^i_{TE_1}(x, y)\right), 0 \leq i \leq K \tag{7}$$

2.2. Dynamic distortion correction during the interventional procedure

The parameterized magnetic field model ΔB^i_0 and the set of parameters D^i_t representing the actual organ displacement allow the reconstruction of the magnetic field distribution corresponding to the current organ position (see Eq. (8)), which can be converted into pixel shifts in phase encoding direction with Eq. (1).

$$\Delta B_0(x, y) = \sum_{i=0}^{K-1} D^i_t \Delta B^i_0(x, y) + \Delta B^K_0(x, y), 0 \leq t < N \tag{8}$$

2.3. Experimental setup

The proposed distortion correction method was evaluated on a data set presented in [13] for comparison, with the permision of the corresponding journal and authors.

In order to evaluate the possibility to obtain distortion-corrected EPI images in real time, dynamic MR-imaging was performed under free-breathing conditions on the abdomen of a healthy volunteer (sagitally positioned single-shot EPI-sequence, four-channels receive coil, echo-train length = 81, repetition time= 78 ms, $TE_1 =$ 39 ms, $TE_2 = 46$ ms, 121 water selective binomial excitation, flip angle= 25°, BWpe= 14.1 Hz, voxel size=$2.7 \times 2.7 \times 7$ mm^3). The volunteer was instructed to breathe using the maximal pulmunary

volume during 20 seconds and normally during another period of 20 seconds. An undistorted steady-state free precession (SSFP) image [18] acquired at the apex of the exhalation phase with the same image geometry and a two-fold increased image resolution was used as a gold standard for the evaluation of the correction. Our test platform was a dual processor (3.1 Ghz Penryn, four cores, INTEL Santa Clara, USA) workstation with 8 GB of RAM.

3. RESULTS

Fig. 1a displays the high-resolution SSFP image of the abdominal organs used as a reference image. Fig. 1b shows the local distortion field in phase-encoding direction (anterior-posterior) calculated using the proposed method. The overlaid anatomical reference points of the uncorrected image and the corrected image in Fig. 1c and 1d demonstrate the effectiveness of the correction. In all images, the boundary of the liver (see arrow I in Fig. 1c and the major vessels in the centre of the liver, which are shifted in the uncorrected data, are remapped to their correct position by the proposed method. Note that the distortion can exceed a magnitude of 1 cm, especially in the interface lung/liver and in vessels in the centre of the liver.

Fig. 2a shows the time evolution of the displacement estimated in the head-foot direction using the PCA-based registration in a single pixel located in the upper part of the liver (red arrow in Fig. 1d). The shift correction is shown to vary by up to 1 mm between two successive acquisitions with the traditional "direct" approach, as shown in Fig. 2b. It can be observed that the noise on the shift correction is strongly reduced using the proposed approach. It is interesting to note that the distortion varies by 2 mm during respiratory cycle, demonstrating that it has to be corrected by an adaptive strategy.

4. DISCUSSION

Compared to existing "direct" approaches described in [13], the introduction of the preparative learning step allows the following improvements: First, during the intervention only the most recently acquired image is a necessary to derive the current magnetic field estimate, which allows:

- To remove the imprecision in the magnetic susceptibility field estimates, which are introduced by the sliding window technique (i.e. $\varphi_{TE_1(n-1)}$, $\varphi_{TE_2(n)}$ and $\varphi_{TE_1(n+1)}$) used in Eq. (3) during periods of rapid acceleration during the motion cycle, as shown in Fig. 2.
- To reduce the latency of the correction compared to direct approaches, which intrinsically rely on a temporal window of past measurements (the original method proposed in [13], based on Eq. (3), has a latency of one image). This is advantageous if the MR-images are used to retroactively control of the interventional procedure in real-time [3]. This also renders the proposed method compatible with 3D multi-slice protocol, since the precision of the correction is not affected by the reduced frame-rate per slice, which is associated with a larger spatial coverage.

Second, the preparative learning step permits the use of magnetic susceptibility field model for the calculation of the EPI-corrections, which is in turn based on a parametric motion model. The parametric motion model allows to maintain only the principal physiological components of the estimated motion, and thus reduces the noise on the estimated displacements (see [14] for more details) and thus in the derived computed magnetic field maps.

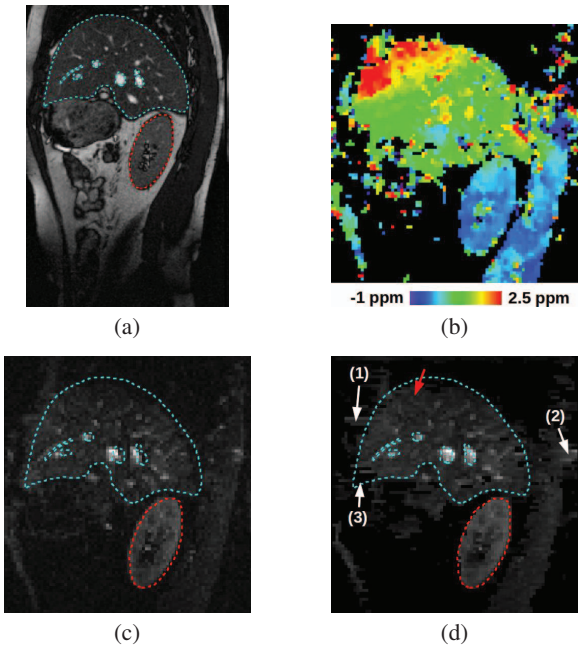


Fig. 1. Example of result extracted from the temporal series. (a): SSFP image of the abdominal organs used as a reference image, (b): local distortion field in phase-encoding direction calculated using the proposed method (1 ppm corresponds to 4.5 mm for the employed sequence, using Eq. (1)), (c): distorted image, (d): distortion-corrected image obtained using the proposed approach. This figure was generated using the data set employed in [13]. This material is reproduced with permision of John Wiley&Sons, Inc.

The resulting improvement of the precision of the shift correction shown in Fig. 2b.

On the other hand, although the model based "indirect" approach improves the precision of the previously suggested "direct" approach for real-time distortion correction, it introduces several new limitations: First, since magnetic field variations are "learned" and subsequently applied to correct geometric distortions during the intervention, the method can intrinsically not correct for distortion artifacts associated with susceptibility perturbation which were absent during the learning step (as for example perturbation induced by the passage of digestive gases due to the peristaltic transport in the digestive tubes).

In addition, in the proposed method the magnetic field perturbation was estimated assuming a simple linear magnetic field variation with organ displacement. Although this assumption has been found valid for small displacements [14], the precision of this simplification must be carefully evaluated in regions displaying large motion amplitudes or large susceptibility variations. In such regions, the correction method will not only fail, but can also lead to increased distortions (see arrows (1), (2) and (3) in Fig. 1d). These points need to be investigated in future studies.

5. CONCLUSION

Interventional real time MR-guidance of non-invasive procedures generally requires a precise representation of the true target object position in the continously acquired images. This is complicated

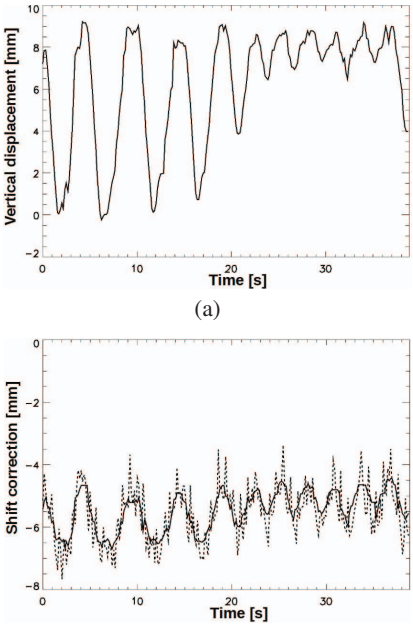


Fig. 2. (a): Time evolution of the displacement estimated in the head-foot direction using the PCA-based registration in a single pixel located in the upper part of the liver (red arrow in Fig. 1d), (b): corresponding shift correction obtained with the traditional "direct" approach (dashed line) and with the proposed method (solid line). This figure was generated using the data set employed in [13]. This material is reproduced with permision of John Wiley&Sons, Inc.

by the frequent presence of dynamic geometric image distortions, in particular when gradient recalled MRI is employed. The proposed geometric distortion correction technique allows a robust real-time correction of this effect for each new acquired image. The low computation time (less than 20ms for the correction of a single slice on our test platform) renders the method compatible with sub-second MRI and does not increase the image processing latency, which are for real-time interventional imaging of great importance. Existing approaches require a high temporal sampling density of the observed motion during the intervention [13] for a precise distortion correction, which generally leads to a compromized spatial coverage of the targeted area. In comparison, the proposed correction approach is independant of the imaging frame-rate and thus fully compatible with multi-slice imaging protols for increased spatial coverage in slice direction.

6. REFERENCES

[1] G. D. Dodd, M. C. Soulen, R. A. Kane, T. Livraghi, W. R. Lees, Y. Yamashita, A. R. Gillams, O. I. Karahan, and H. Rhim, "Minimally invasive treatment of malignant hepatic tumors: at the threshold of a major breakthrough," *Radiographics*, vol. 20(1), pp. 9–27, 2000.

[2] M. Ries, B. Denis de Senneville, S. Roujol, Y. Berber, B. Quesson, and C.T.W. Moonen, "Real-time 3D target tracking in mri guided focused ultrasound ablations in moving tissues," *Magnetic Resonance in Medicine*, vol. 64(6), pp. 1704–1712, 2010.

[3] C. Mougenot, B. Quesson, B. Denis de Senneville, P. Loureno de Oliveira, S. Sprinkhuizen, J. Palussière, N. Grenier, and C.T.W. Moonen, "Three dimensional spatial and temporal temperature control with MR-thermometry guided focused ultrasound," *Magnetic Resonance in Medicine*, vol. 61(3), pp. 603–614, 2008.

[4] E. M. Haacke, R. W. Brown, M. R. Thompson, and R. Venkatesan, "Magnetic resonance imaging: Physical principles and sequence design," in *Wiley-Blackwell*, 1999.

[5] P. Mansfield, "Multi-planar image formation using NMR spin echoes," *J Phys C*, vol. 10, pp. 50–58, 1977.

[6] K.P. Pruessmann, M. Weiger, M.B. Scheidegger, and P. Boesiger, "SENSE: sensitivity encoding for fast mri," *Magnetic Resonance in Medicine*, vol. 42, pp. 952–962, 1999.

[7] J. De Poorter, C. De Wagter, Y. De Deene, C. Thomson, F. Stahlberg, and E. Achten, "The proton resonance frequency shift method compared with molecular diffusion for quantitative measurement of two dimensional time dependent temperature distribution in phantom," *Journal of Magnetic Resonance Imaging*, vol. 103, pp. 234–241, 1994.

[8] B. Denis de Senneville, C. Mougenot, and C.T.W. Moonen, "Real time adaptive methods for treatment of mobile organs by MRI controlled high intensity focused ultrasound," *Magnetic Resonance in Medicine*, vol. 57(2), pp. 319–330, 2007.

[9] P.J. Reber, E.C. Wong, R.B. Buxton, and Franck L.R., "Correction of off resonance-related distortion in echo-planar imaging using EPI-based field maps," *Magnetic Resonance in Medicine*, vol. 39, pp. 328–330, 1998.

[10] Q.S. Xiang and F.Q. Ye, "Correction for geometric distortion and n/2 ghosting in EPI by phase labeling for additional coordinate encoding (PLACE)," *Magnetic Resonance in Medicine*, vol. 57, pp. 731–741, 2007.

[11] P. Jezzard and R.S. Balaban, "Correction for geometric distortion in echo planar images from b0 field variations," *Magnetic Resonance in Medicine*, vol. 34, pp. 65–73, 1995.

[12] H. Zeng and R.T. Constable, "Image distortion correction in EPI: comparison of field mapping with point spread function mapping," *Magnetic Resonance in Medicine*, vol. 48, pp. 137–146, 2002.

[13] I. Dragonu, B. Denis de Senneville, B. Quesson, C.T.W. Moonen, and M. Ries, "Real-time geometric distortion correction for interventional imaging with EPI," *Magnetic Resonance in Medicine*, vol. 61(4), pp. 994–1000, 2008.

[14] B. Denis de Senneville, M. Ries, G. Maclair, and C.T.W. Moonen, "MR-guided thermotherapy of abdominal organs using a robust PCA-based motion descriptor," *Transaction on Medical Imaging*, vol. 30(11), pp. 1987–1995, 2011.

[15] J.B. Maintz and M.A. Viergever, "A survey of medical image registration," *Med Image Anal*, vol. 2(1), pp. 1–36, 1998.

[16] B.K.P. Horn and B.G. Schunck, "Determining optical flow," *Artificial intelligence*, vol. 17, pp. 185–203, 1981.

[17] I. Pratikakis, C. Barillot, P. Hellier, and E. Memin, "Robust multiscale deformable registration of 3D ultrasound images," *International Journal of Image and Graphics*, vol. 3(4), pp. 547–566, 2003.

[18] H.Y. Carr, "Steady-state free precession in nuclear magnetic resonance," *Phys Rev*, vol. 112, pp. 16931701, 1958.